Electronic Supplementary Material (ESI) for Physical Chemistry Chemical Physics.

Supplementary Information: Temperature and collision energy effects on dissociation of hydrochloric acid on water surfaces

Lauri Partanen,*,† Garold Murdachaew,† R. Benny Gerber,†,‡,¶ and Lauri Halonen†

†*Laboratory of Physical Chemistry, Department of Chemistry, P.O. Box 55 (A.I. Virtasen aukio 1), FIN-00014 University of Helsinki, Finland*

‡*Institute of Chemistry and the Fritz Haber Research Center, The Hebrew University, Jerusalem 91904 Israel*

¶*Department of Chemistry, University of California Irvine, Irvine, California 92697, United States*

E-mail: lauri.partanen@helsinki.fi

1 Supplementary Material

1.1 Characteristics of the simulation slab

The calculated O-O radial distribution functions (RDFs) g_{OO} of the bulk at 390, 300, and 212 K together with the latest experimental results by Soper[1] are displayed in Figure S1 together with the RDFs obtained from the bulk region of our water slabs at these temperatures. To compare the two, the slab RDFs were renormalized by the normalization factor of the bulk $N_{\mathrm{b}}^2 V_{\mathrm{s}}/N_{\mathrm{s}}^2 V_{\mathrm{b}}$ where N is the number of atoms in the bulk or surface simulation and V is the

volume of the simulation box. Out of the different RDFs, we chose to focus on g_{OO} because it is the least affected by nuclear quantum effects.[2] When compared with the most recent X-ray diffraction results from Skinner, where the first peak is located at about 2.80 Å and has a height of 2.57 and the second peaks is found at 4.5 Å with a height of 1.12,[3] it is seen that BLYP-D2/DZVP still produces an overstructured RDF profile at 300 K, as expected. Compared to the 300 K results, the 390 K results of both the slab and the bulk calculation are significantly closer to the neutron diffraction results of Soper measured at 298 K,[1] in line with the melting point studies of Yoo and Xantheas.[4] On the other hand, as can be seen from Figure S1 at 212 K the peaks of both the bulk and the slab calculation become significantly sharper when compared to 300 K indicating a more ice-like structure. While the slab results are in qualitative agreement with experiment, there are clear differences between the radial distributions obtained from the bulk region of our slab and the actual bulk calculations, which indicate that the central regions of our slab show only approximate bulk behaviour. Especially in the case of the 212 K slab, the second peak is shifted to the left in line with the higher densities obtained from our calculations for the bulk region of the slab at all temperatures.

The parameters ρ_{l}, z_{GDS}, and δ obtained by fitting Equation (1) of the main text to the density profile are in Table S1. Here, the 300 K δ parameter value is in agreement with the values obtained by Kuo et al. with BLYP/TZV2P in their paper with a 216 water slab.[5] While BLYP alone generally yields lower densities than expected for water, which then become a little too high after diffusion is accounted for by the Grimme correction , in our results the shifting of the g_{OO} function to the left seen in Figure S1 is reflected in the higher density values obtained from the fit and confirms that the central regions of the slab behave only approximately as bulk water due to the size of the slab employed in the calculations.

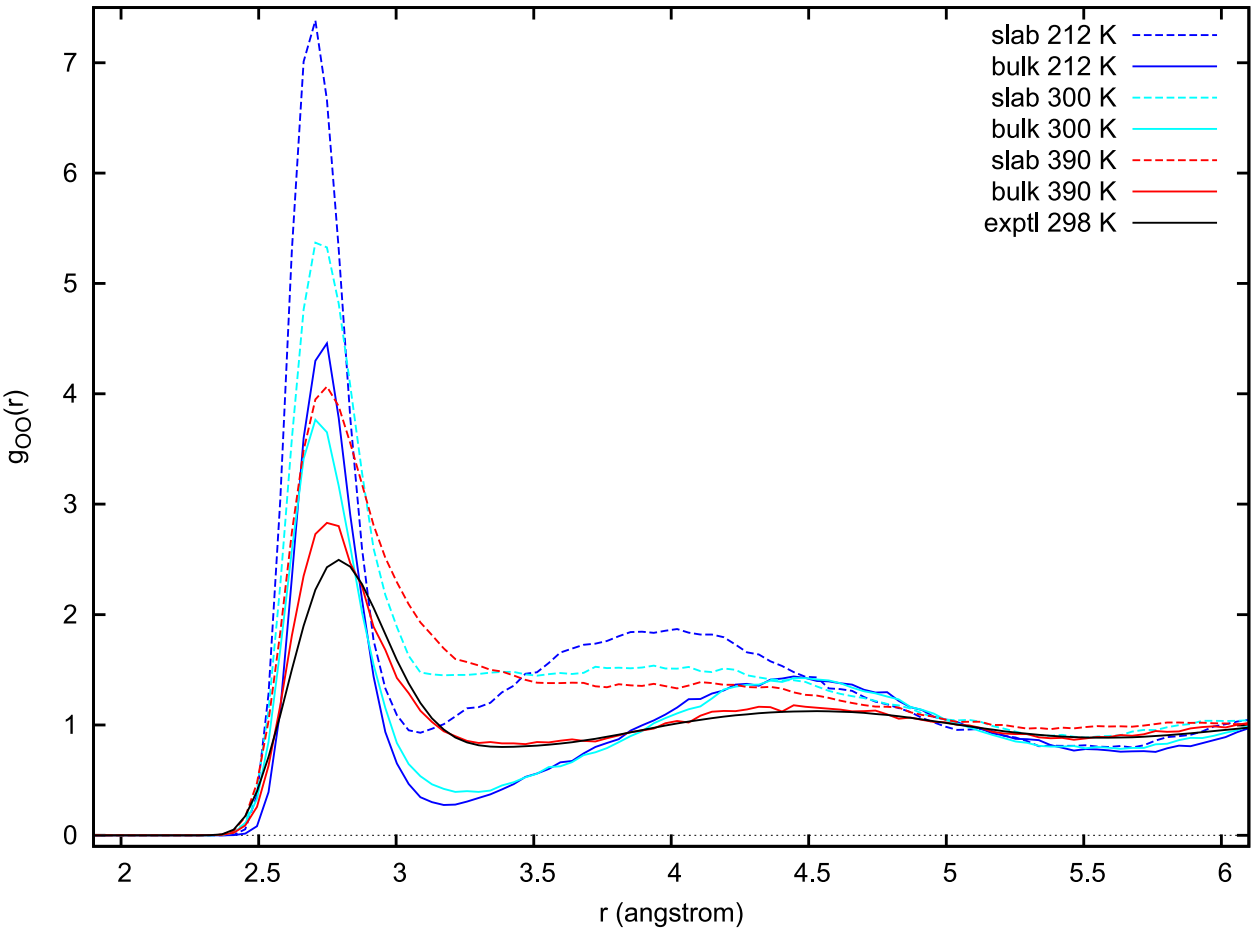

Figure S1: The g_{OO} -radial distribution function for the bulk and bulk region of the slab at different temperatures compared with experiment. The bulk RDFs are represented by solid lines, while RDFs in the bulk regions of the slab are given by dashed lines.

Table S1: Gibbs dividing surface locations, δ values and bulk slab densities at different temperatures

T / K	z_{GDS}/Å	δ/Å	$\rho_{\mathrm{l}}/(\mathrm{g/cm^{-3}})$
212	4.15	0.98	1.22
300	4.45	0.86	1.14
390	4.48	0.81	1.14

1.2 Additional Discussion on the Methods

In terms of the basis set size adopted in this study, the fact that our bulk g_{OO} peak positions are in close agreement with those obtained by Baer et al. using the same functional and the larger TZV2P basis set in the bulk region of a 216 water molecule slab,[6] indicates that DZVP is a viable alternative when a large number of trajectories need to be calculated. In addition to ours, several previous studies used dispersion-corrected BLYP with a DZVP-sized basis set.[7–11] For example, utilizing exactly the same BLYP-D2/DZVP method as us, Murdachaew et al.[9] found good agreement in terms of geometries and a tolerable 15 % difference in adsorption energies per water molecule compared to BLYP-D2/TZV2P in their study on the deprotonations of H_2SO_4 in an aqueous system. In their study on the dissociation of HCl in the same aqueous system, they found that DZVP combined with BLYP-D reproduced well the adsorption energies of a single HCl or water molecule to the dry, hydroxylated silica surface and structures obtained with larger basis sets up to molopt-TZV2P.[8] With regard to the BLYP(-D2) functional used in this study, while generalized gradient (GGA) exchange and correlation functionals (XCFs) have been widely used for studying proton transfer reactions,[12–14] due to self-interaction error for these reactions GGA XCFs underestimate the proton-transfer barrier.[15–17] As a result, the obtained proton transfer rates are exaggerated and can be treated at most semi-quantitatively correct. While hybrid functional methods are available to overcome most of these shortcomings,[15] the computational costs associated with hybrid methods make them unattractive to proton transfer processes in extended systems.[18]

1.3 Scattering at 0° angle at 300 K

The scattering results with $4kT$ kinetic energy at a 0° angle with respect to the surface anti-normal are shown in Figure S2. Two of the trajectories behave identically to the ones depicted in panel (b) of Figure 3 of the main text, showing dissociation times below 2 ps, signifying a dissociation virtually upon impact with the slab. This observation combined with the fact that the trajectories that are most likely to dissociate rapidly in thermal

collisions are the ones that have the largest amount of energy normal to the surface at the beginning of the calculation indicate that the reaction on the surface is mostly dependent on the energy normal to the surface. The third, blue trajectory shows a recoil where the HCl molecule as a whole first penetrates almost into the bulk and then bounces back to the surface where it dissociates after about 4 ps. This behaviour was not observed in our 45° scattering trajectories, although some small recoil is visible in few of the trajectories in panels (a) and (b) of Figure 8 of the main text.

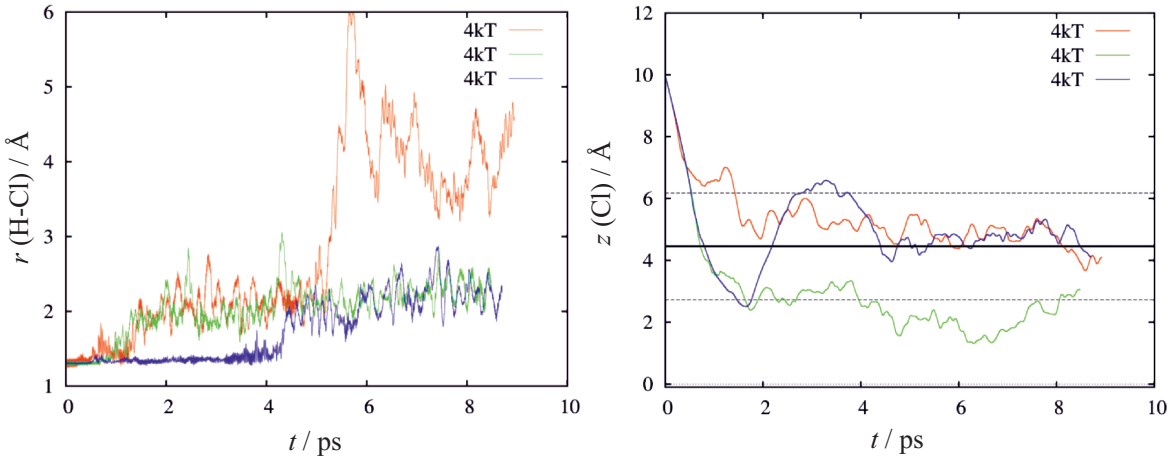

Figure S2: The H-Cl bond distance and the z component of the Cl atom as a function of time with an incidence angle of 0°.

References

(1) Soper, A. K. *ISRN Phys. Chem.* **2013**, *2013*, 279463.

(2) Lin, I. C.; Seitsonen, A. P.; Tavernelli, I.; Rothlisberger, U. *J. Chem. Theory Comput.* **2012**, *8*, 3902–3910.

(3) Skinner, L. B.; Huang, C.; Schlesinger, D.; Pettersson, L. G. M.; Nilsson, A.; Benmore, C. J. *J. Chem. Phys.* **2013**, *138*, 074506.

(4) Yoo, S.; Xantheas, S. S. *J. Chem. Phys.* **2011**, *134*, 121105.

(5) Kuo, I. -F. W.; Mundy, C. J.; Eggimann, B. L.; McGrath, M. J.; Siepmann, J. I.; Chen, B.; Vieceli, J.; Tobias, D. J. *J. Phys. Chem. B* **2006**, *110*, 3738–3746.

(6) Baer, M. D.; Mundy, C. J.; McGrath, M. J.; Kuo, I. -F. W.; Siepmann, J. I.; Tobias, D. J. *J. Chem. Phys.* **2011**, *135*, 124712.

(7) Hammerich, A. D.; Buch, V. *J. Phys. Chem. A* **2012**, *116*, 5637–5652.

(8) Murdachaew, G.; Gaigeot, M. -P.; Halonen, L.; Gerber, R. B. *J. Phys. Chem. Lett.* **2013**, *4*, 3500–3507.

(9) Murdachaew, G.; Gaigeot, M. -P.; Halonen, L.; Gerber, R. B. *Phys. Chem. Chem. Phys.* **2014**, *16*, 22287–22298.

(10) Riikonen, S.; Parkkinen, P.; Halonen, L.; Gerber, R. B. *J. Phys. Chem. Lett.* **2013**, *4*, 1850–1855.

(11) Riikonen, S.; Parkkinen, P.; Halonen, L.; Gerber, R. B. *J. Phys. Chem. A* **2014**, *118*, 5029–5037.

(12) Marx, D.; Tuckerman, M. E.; Hutter, J.; Parrinello, M. *Nature* **1999**, *397*, 601–604.

(13) Marx, D. *Chem. Phys. Chem.* **2006**, *7*, 1848–1870.

(14) Kulig, W.; Agmon, N. *Nat. Chem.* **2013**, *5*, 29–35.

(15) Nachimuthu, S.; Gao, J.; Truhlar, D. G. *Chem. Phys.* **2012**, *400*, 8–12.

(16) Sadhukhan, S.; Muñoz, D.; Adamo, C.; Scuseria, G. E. *Chem. Phys. Lett.* **1999**, *306*, 83–87.

(17) Barone, V.; Orlandini, L.; Adamo, C. *Int. J. Quantum Chem.* **1995**, *56*, 697–705.

(18) Guidon, M.; Hutter, J.; VandeVondele, J. *J. Chem. Theory Comput.* **2009**, *5*, 3010–3021.